

The imaging of cartilaginous bone tumours. II. Chondrosarcoma

H. Douis · A. Saifuddin

Received: 17 June 2012 / Revised: 27 August 2012 / Accepted: 30 August 2012 / Published online: 4 October 2012
© ISS 2012

Abstract Chondrosarcoma is the third most common primary malignant bone tumour. There are various histological subtypes of chondrosarcomas, of which conventional intramedullary chondrosarcoma is by far the most common. Rarer sub-types include clear cell chondrosarcoma, myxoid chondrosarcoma, mesenchymal chondrosarcoma and dedifferentiated chondrosarcoma. Chondrosarcoma is also classified into central, peripheral and periosteal, dependent upon the lesion site, and into primary chondrosarcoma if the lesion arises de novo and secondary chondrosarcoma if the tumour arises in a pre-existing lesion. The various subtypes of chondrosarcoma have characteristic imaging features that may aid diagnosis and may guide biopsy, therefore potentially preventing misdiagnosis. The aim of this article is to provide an overview of the pertinent clinical and imaging findings of the different forms of chondrosarcoma.

Keywords Conventional intramedullary chondrosarcoma · Clear cell chondrosarcoma · Mesenchymal chondrosarcoma · Dedifferentiated chondrosarcoma · Periosteal chondrosarcoma · Secondary chondrosarcoma · Imaging

Introduction

Chondrosarcoma (CS) represents a malignant tumour of cells that produce a cartilaginous matrix [1–5]. Overall, CS accounts for ~3.5% of all biopsied primary bone tumours and 20–27% of all primary bone sarcomas, being the third commonest after myeloma and osteosarcoma.

Chondrosarcoma may be classified as primary or secondary. Primary CS arises de novo, while secondary CS arises in association with a pre-existing cartilaginous lesion, such as enchondroma or osteochondroma [6, 7], and also includes those complicating enchondromatosis (Ollier's disease, Maffucci syndrome) [8] and hereditary multiple exostoses (HME, diaphyseal aclasis) [9]. Lesions are also classified according to their site as being central, peripheral or juxtacortical. Central CS arises within the medullary cavity, peripheral CS arises within the cartilage cap of an osteochondroma, while juxta-cortical or periosteal CS arises on the surface of the bone.

The further classification of CS is based on the various histological subtypes, which include conventional intramedullary (Grades 1–3), clear cell, myxoid, mesenchymal and dedifferentiated [4, 5].

Conventional intramedullary chondrosarcoma

Central CS is the commonest type, representing a tumour of malignant chondrocytes that can be differentiated histologically into three grades: grade 1 (low-grade), grade 2 (intermediate) and grade 3 (high-grade). Grade 1 is the commonest and can be difficult to differentiate from enchondroma, the presence of entrapment and destruction of the surrounding host bone being the hallmark of the lesion [5]. The difficulties that clinicians, radiologists and pathologists face in the differentiation of enchondroma from low-grade chondrosarcoma and the difficulty in the histological grading of chondrosarcoma have been emphasized in two recent studies that evaluated the interobserver variability in the diagnosis and histological grading of cartilaginous tumours. Both studies demonstrated low reliability in the distinction between enchondroma and low-grade chondrosarcoma and a low reliability in the histological grading of

H. Douis (✉) · A. Saifuddin
Department of Radiology,
The Royal National Orthopaedic Hospital NHS Trust,
Brockley Hill,
Stanmore, Middlesex HA7 4LP, UK
e-mail: douis.hassan@gmx.de

chondrosarcoma amongst bone tumour pathologists [10, 11]. Furthermore, the SLICED (Skeletal Lesions Interobserver Correlation among Expert Diagnosticians) study group also demonstrated significant variation among radiologists in differentiating enchondroma from low-grade chondrosarcoma and a low reliability in the grading of chondrosarcoma based on radiography or computed tomography, with slightly improved agreement amongst radiologists when MRI was used [10]. As mentioned in the first part of this series, it is therefore vital that the differentiation of benign from malignant cartilage tumours is based on a decision made in a multidisciplinary team that takes into account the clinical, imaging and pathology findings.

In clinical practice, grade 1 chondrosarcoma is the most commonly observed. In a study of 101 uncomplicated central CS, 53 tumours were grade 1, 40 tumours were grade 2 and only 8 were grade 3 [12].

Central CS typically presents in the 4th to 5th decades of life and is 1.5–2 times commoner in male subjects [5]. Pain is the presenting complaint in 95% of cases, with a palpable soft tissue mass or fullness described in 28–82%. In 3–17%, presentation is with pathological fracture.

The long bones of the appendicular skeleton are the commonest sites for central CS (45% of cases), most commonly the femur (20–35%), tibia (5%) and the upper limb (10–20%), in which case the humerus is the most frequent site. Involvement of the axial skeleton is also relatively common, with 25% of tumours involving the innominate bone, 8% the ribs, 5% the scapula and 2% the sternum. However, almost any bone can be involved, including the small bones of the hands [13] and feet [14].

Within the long bones, approximately 50% affect the metaphyseal region and 36% the diaphysis [5]. Epiphyseal central CS is reported in 16% of cases, while subarticular extension has also been recorded [15]. Lesions of the femur, tibia, humerus and fibula are most commonly located proximally.

The routine pre-operative staging of sarcomas in general, including chondrosarcoma of bone, involves MRI of the affected area for loco-regional staging, computed tomography of the chest to assess the presence of pulmonary metastases and Tc-99m MDP bone scintigraphy to evaluate the presence of skeletal metastases. However, the role of skeletal scintigraphy in the initial staging of chondrosarcoma of bone has recently been challenged by Douis et al., who retrospectively evaluated the bone scintigraphy reports of 188 patients with chondrosarcoma of bone at initial surgical staging. The authors did not find any skeletal metastases due to chondrosarcoma at initial presentation. However, they identified 3 patients with multifocal chondrosarcomas, 2 of whom had known Ollier's disease and would have been adequately imaged on the initial MR staging study, whilst

the third patient with multifocal chondrosarcoma was found to have a presumed low-grade central chondrosarcoma in the opposite femur. However, this unexpected finding in the third case depicted on skeletal scintigraphy did not change the surgical management as the lesion was observed and remained unchanged. Therefore, the authors concluded that there is little role for the use of skeletal scintigraphy in the initial surgical staging of chondrosarcoma of bone [16].

Surgical management of central CS is primarily dependent upon histological grade [2]. Grade 1 CS can be successfully treated with intralesional curettage [17], while grade 2 and above are managed by wide excision and endoprosthesis replacement when limb salvage is possible, as is typically the case [2].

Outcome is largely dependent upon histological grade, surgical margins and staging. Grade 1 CS is rarely associated with metastases at presentation [18]. The overall 5-year survival rate for conventional central CS is reported to be 76% [19]. Local recurrence following treatment of grade 1 central CS is associated with higher histological grade of the recurrence, an increased risk of metastases and reduced survival [20]. Outcome may also be influenced by lesion site, with an overall 5-year survival of 92% in chest wall CS [21], 83% in scapular CS [22] and 59% in pelvic CS [23],



Fig. 1 Central low-grade chondrosarcoma. Lateral radiograph shows a mixed lytic and sclerotic lesion in the distal femur (arrows), which demonstrates the typical ring-and-arc chondral-type matrix mineralisation

while local recurrence is reported to be commoner in pelvic [24] and scapular tumours [25]. Interestingly, a recent study that analysed 2,890 CS from the SEER (Surveillance, Epidemiology and End Results) database found that on multivariate analysis, histological grading and surgical staging were independent prognostic factors for survival in CS, whilst tumour location was only associated with a difference in survival on univariate analysis with appendicular CS being associated with a better overall survival rate than axial CS [26]. However, this study did not perform a subgroup

analysis of CS located in different parts of the axial skeleton. Similarly, a study by Bramer et al. revealed that the presence of a pathological fracture in CS was not associated with an increased risk of local recurrence and was not a predictor of survival in CS [27].

Radiographs of central long bone CS typically show a region of mixed lysis and sclerosis, the sclerotic areas representing classical rings and arcs of chondral matrix mineralisation (Figs. 1, 2), which are seen in 60–78% of cases [5]. The degree of calcification is very variable (Fig. 3), but

Fig. 2 Central low-grade chondrosarcoma. **a** Anteroposterior (AP) radiograph of the knee shows a predominantly sclerotic lesion in the proximal tibia (*arrows*), which reveals the characteristic ring-and-arc chondral-type matrix mineralisation. **b** Axial CT study exquisitely depicts the degree of endosteal scalloping of the cortex (*arrow*), which is not appreciated on the radiograph. **c** Coronal T1W FSE MR image shows the classical lobular appearance of chondrosarcoma. The lesion has low-to-intermediate signal intensity (SI) with areas of signal void due to matrix mineralisation (*arrows*) and areas of high signal intensity due to entrapped medullary fatty marrow (*arrowheads*). Note the small cartilaginous lesion within the mid-shaft of the tibia, which most likely represents an enchondroma. **d** Axial fat-suppressed T2W FSE MR image clearly reveals the depth and extent of endosteal scalloping

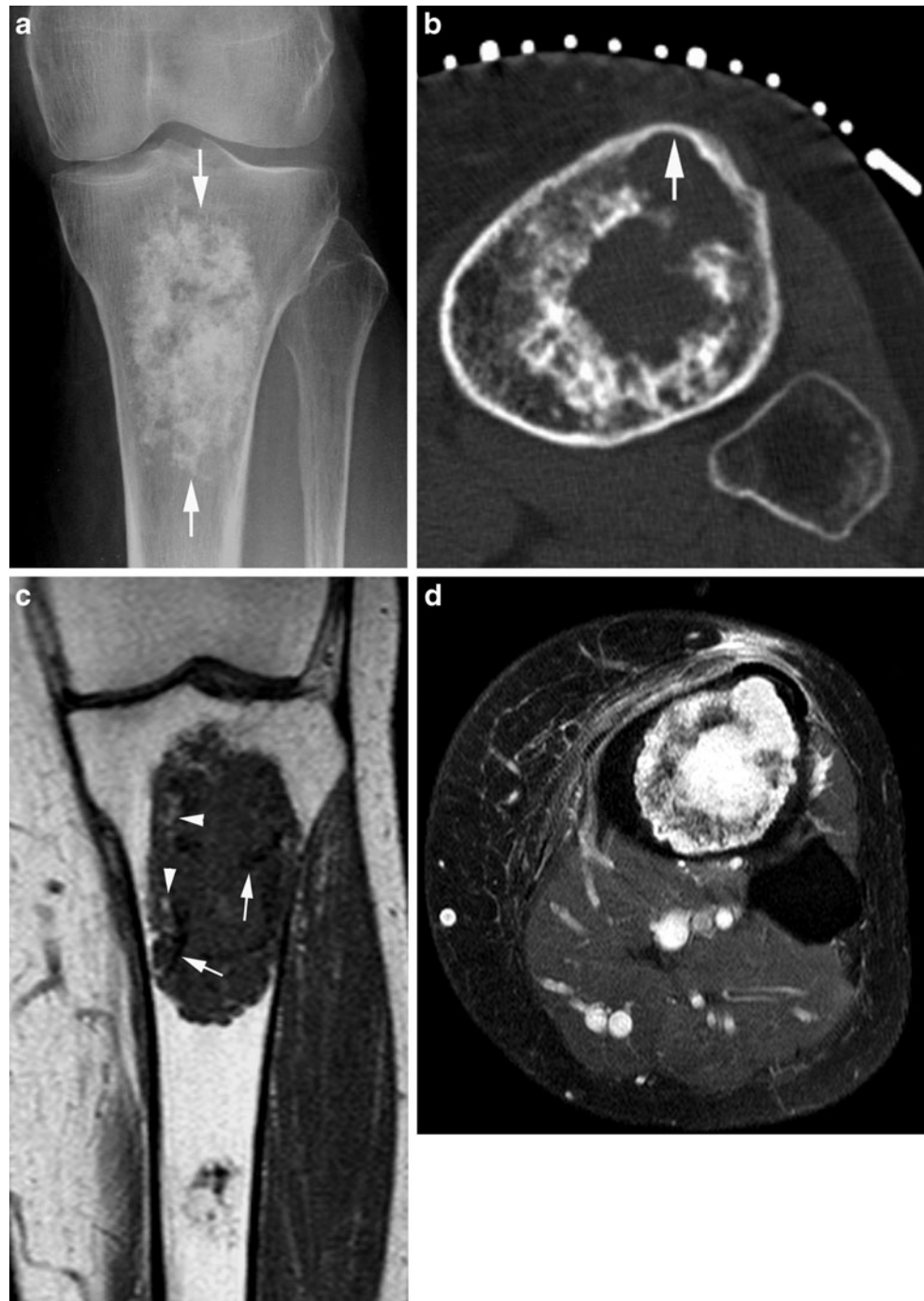


Fig. 3 Central low-grade chondrosarcoma. **a** AP radiograph of the wrist demonstrates a central chondrosarcoma (arrows) of the distal radius with no appreciable matrix mineralisation. **b** Coronal fat-suppressed T1W FSE MR image with contrast medium demonstrates septal and peripheral enhancement of the lesion and the classical lobular appearance of chondrosarcoma. Note the presence of endosteal scalloping, which is visible on the radiograph and MR image (arrow)



higher grade tumours tend to show less mineralisation (Fig. 4). Low-grade tumours classically demonstrate a geographic, lobular margin, while moth-eaten or permeative bone destruction is indicative of higher grade lesions (Fig. 5) or possible dedifferentiation. As the lesion grows, it causes lobular endosteal scalloping (Fig. 3a), which may progress to cortical expansion, cortical penetration (Fig. 6; seen in ~60% of cases on radiography) and a soft-tissue mass (seen in ~50% of cases on radiography). Deep endosteal scalloping (>two thirds of the depth of the cortex) is a sensitive discriminator between central CS and enchondroma. Cortical remodelling, cortical thickening and periosteal reaction are also much more suggestive of central CS (Fig. 7). Central CS is almost always greater than 4 cm in size, and 50% of long bone cases may be greater than 10 cm in length, occupying from 30 to 50% of the whole bone length.

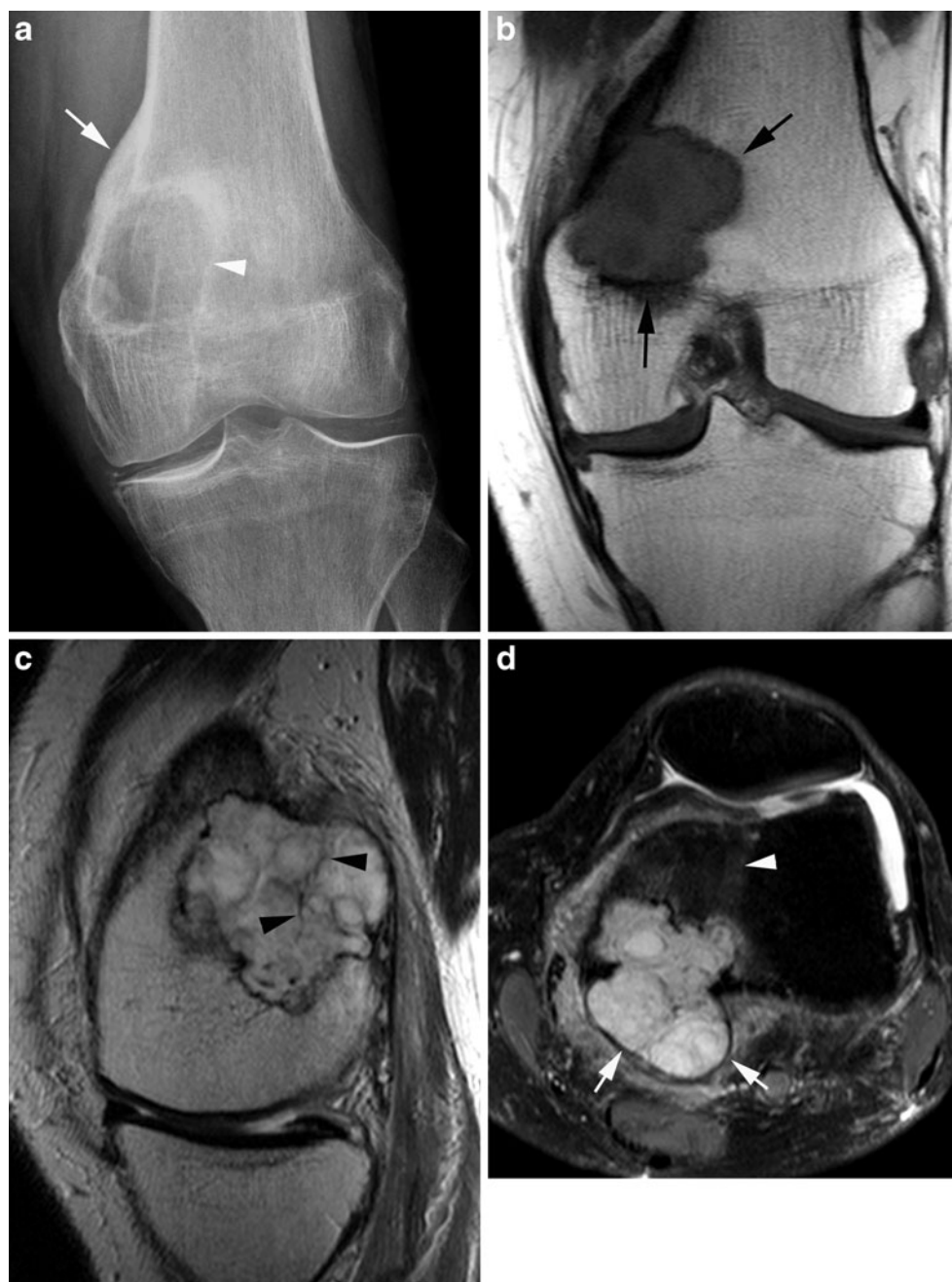
99m-Tc MDP bone scintigraphy shows irregular focal increased activity, which is greater than that of the iliac crest, in over 80% of cases (Fig. 7b), which helps to distinguish the lesion from enchondroma, where the activity level is typically less than that of the iliac crest. However, in a study looking at CS of the rib, there was no correlation between degree of activity and histological grade [28].

The role of [18F] fluoro-2-deoxy-D-glucose positron emission tomography (18FDG-PET) in the differentiation of benign from malignant cartilage neoplasms has also been investigated. Feldman et al. evaluated the role of 18FDG-PET in differentiating benign from malignant cartilage neoplasms. In their study, 29 patients with cartilaginous lesions (patients with enchondromas, osteochondromas, peripheral,

central and extraskeletal chondrosarcomas) underwent 18FDG-PET of which 26 patients underwent surgery. They found that a cut-off value for the maximum SUV of 2.0 was able to differentiate benign from malignant cartilaginous lesions with a sensitivity of 90.9%, a specificity of 100% and accuracy of 96.6% [29]. However, because of the heterogeneous study group, the small sample size and the inclusion of patients with high-grade chondrosarcomas, it is difficult to draw conclusions about the value of 18FDG-PET in differentiating benign cartilaginous lesions, particularly enchondromas from low-grade chondrosarcomas. 18FDG-PET has also proved to be of value in the differentiation of histological grade of central CS, and in the prediction of tumours that are more likely to recur [30].

Computed tomography features that may not be radiographically evident include occult matrix mineralisation, and a better appreciation of the depth and degree of endosteal scalloping (Fig. 2b). Over 90% of long bone CS will show calcification on CT. Focal areas of endosteal scalloping greater than two thirds of the depth of the cortex are seen in 90% of cases (only 10% in enchondroma), and the longitudinal extent of the lesion showing deep endosteal scalloping is also far greater on CT, involving the whole length of the tumour in ~80% of cases [5]. Cortical destruction from endosteal scalloping is reported in 88% of long bone CS and a soft-tissue mass is present in 59% of cases [5]. Soft-tissue masses may show typical matrix mineralisation and relatively low CT attenuation owing to the high water content of low-grade CS. Septal and rim enhancement can be seen following intravenous contrast medium administration. Higher grade CS may show greater soft tissue extension,

Fig. 4 Conventional intramedullary high-grade chondrosarcoma. **a** AP radiograph of the knee demonstrates a lytic destructive lesion that arises in the distal lateral femur, resulting in cortical thickening, periosteal reaction (*arrow*) and marginal sclerosis (*arrowhead*). Note the relative paucity of matrix mineralisation within the lesion. **b** Coronal T1W FSE MR image shows the lesion to be of intermediate SI leading with associated periosteal reaction and marginal sclerosis (*arrowhead*). **c** Sagittal T2W FSE MR image demonstrates the lesion to be markedly hyperintense with hypointense internal septa (*arrowheads*) and posterior extraosseous extension. **d** Axial fat-suppressed T2W FSE MR image demonstrates cortical destruction, soft-tissue extension (*arrows*) and peri-lesional marrow oedema-like SI (*arrowhead*)



with the mass showing attenuation characteristics closer to those of muscle owing to the increased cellularity of the tumour. For this reason, the tumour typically enhances more uniformly following contrast medium administration.

Magnetic resonance imaging most accurately demonstrates the extent of intraosseous tumour, which classically shows a lobular growth pattern at its margin [5] (Figs. 3b, 4b). The lesion demonstrates low to intermediate T1W SI, possibly with small speckled areas of high SI due to entrapped areas of yellow marrow (35% of cases), and punctate areas of signal void due to matrix mineralisation (Fig. 5c) [5]. The non-calcified areas of tumour show very high T2W

SI because of their high water content, with lobules of chondral tissue being separated by hypointense internal septa (Figs. 4c, 5b). Further areas of heterogeneous low SI are due to matrix mineralisation. Perilesional marrow oedema-like SI is uncommon, but may help differentiate CS from enchondroma (Fig. 8) [5]. As with CT, the depth and extent of endosteal scalloping, extraosseous extension and reactive cortical changes are all clearly observed (Figs. 2d, 4c, 5b, c). Following intravenous contrast medium administration, CS typically shows septal and peripheral enhancement (Fig. 3b). MRI can also be used to differentiate low-grade from high-grade CS. Entrapped fat within the CS

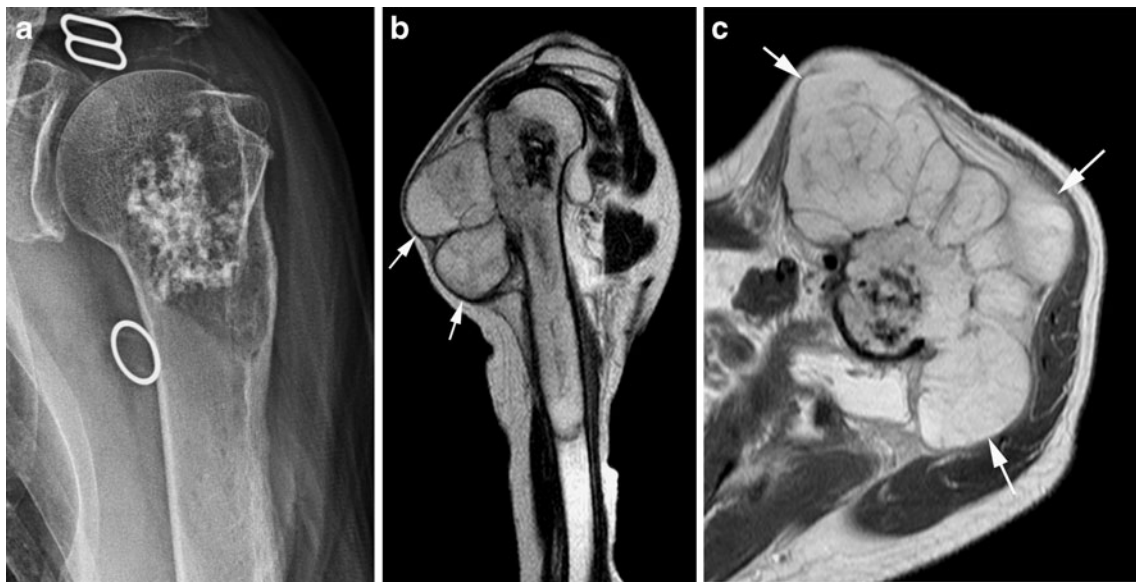


Fig. 5 Grade 2 intramedullary chondrosarcoma. **a** AP radiograph of the left proximal humerus reveals an ill-defined lytic lesion with matrix mineralisation, which demonstrates permeative bone destruction. **b** Sagittal T2W FSE and **c** axial PDW FSE MR images show extensive

cortical destruction and marked soft tissue extension of the lesion (*arrows*)—a finding not appreciated on the radiograph—and also punctate areas of signal void due to matrix mineralisation

strongly suggests a low-grade CS, whilst soft tissue extension is highly indicative of high-grade CS (Figs. 2, 4, 5) [31].

Central pelvic CS most frequently involves the ilium, particularly the region around the site of the fused tri-radiate cartilage (Fig. 9) [5]. Tumours tend to be large at presentation, with CT and MRI commonly demonstrating extensive soft-tissue masses (Fig. 9b, c). Solitary chondral tumours of the sternum (Fig. 10) and ribs are most likely to be chondrosarcomas rather than enchondromas, which are very rare at these sites, with rib lesions most commonly arising anteriorly at the costochondral junction (Fig. 11) [5].

The differentiation between enchondroma and central CS in the small bones of the hands and feet is difficult, with the depth and extent of endosteal scalloping being a poor discriminator [5]. The presence of cortical destruction and soft tissue extension is more suggestive of CS (Fig. 12), as is location in the hindfoot bones (Fig. 13).

Clear cell chondrosarcoma

Clear cell chondrosarcoma (CC-CS) is a tumour characterised by its epiphyseal location in long bones and tumour cells with abundant clear cytoplasm [5, 32, 33]. It is a low-grade lesion accounting for 1–2% of all CS and 0.2% of all biopsied bone tumours [5]. Patients typically present in the 3rd to 5th decades of life and the lesion is twice as common in men. Its particular location results in localised pain and reduced joint motion, with 25% of cases leading to pathological fracture.

The long bones are affected in 85–90% of cases of CC-CS, most commonly the proximal femur (68%) and proximal humerus (23%) [32], while 10–15% occur around the knee [5]. The flat bones are involved in ~10% of cases [5]. The measurement of serum alkaline phosphatase has been proposed as a tumour marker in the diagnosis and follow-up of clear cell chondrosarcoma [34]. Treatment is by wide local resection [34].

Radiologically, CC-CS presents as a predominantly lytic epiphyseal lesion (Fig. 14) with a variable zone of transition and metaphyseal extension [5]. Rarely, extension into the metadiaphysis may occur [32]. In ~20% of cases, a thin sclerotic margin is identified and matrix mineralisation is seen in 30% (Fig. 14a, b). Mild bone expansion is also evident in ~30%, but frank extraosseous extension is rare (<10%) [5]. Proximal humeral lesions may show a more aggressive growth pattern [32]. The thin sclerotic margin, cortical breakthrough and matrix mineralisation are all better appreciated on CT [32].

On MRI [32], the lesion is typically heterogeneous and of low-intermediate T1W SI (Fig. 14c), the heterogeneity resulting from areas of increased SI due to haemorrhage and areas of reduced SI due to mineralisation. Heterogeneous increased SI is seen on T2W and STIR sequences (Fig. 14d), which may show focal areas of brighter SI due to cystic change, possibly with a multilocular appearance or fluid levels. Mineralisation results in focal signal void. Perilesional marrow oedema is unusual and always mild, a feature that helps in the distinction from chondroblastoma [35]. Adjacent soft tissue reactive changes are usually due to an associated pathological fracture.

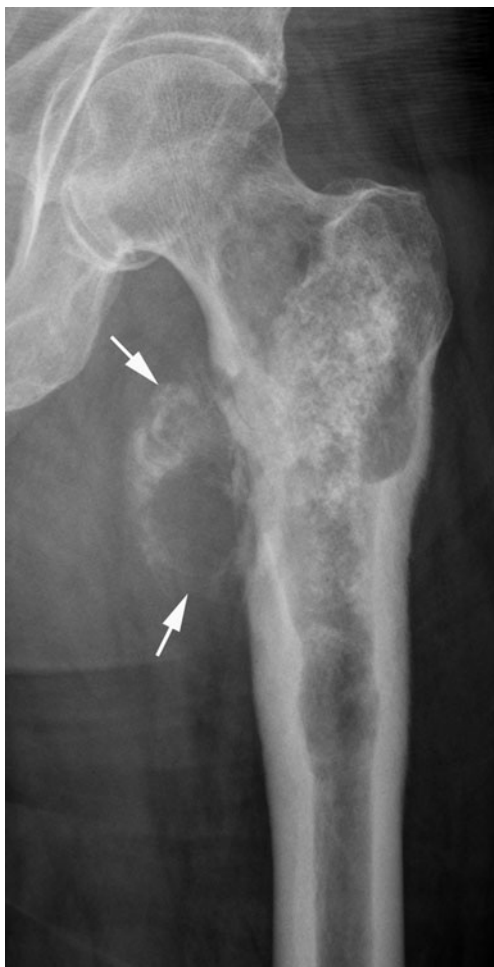


Fig. 6 High-grade intramedullary chondrosarcoma. AP radiograph of the left proximal femur demonstrates an extensive lytic lesion with chondral-type matrix calcification, with associated mineralisation in the extra-osseous component (arrows)

Unusual features include primary diaphyseal location [36] and a more aggressive pattern of behaviour, including early metastases or multiple/synchronous locations [37]. Finally, dedifferentiation has been reported in the association with CC-CS at the time of diagnosis, within local recurrence and in metastatic lesions [38].

Mesenchymal chondrosarcoma

Mesenchymal CS is a rare high-grade variant of CS, which accounts for 2–13% of all bone CS and 5% of all biopsied primary bone tumours. Mesenchymal CS presents in a younger age group than conventional CS, the mean age being ~25 years, and equally commonly in men and women. In the appendicular skeleton, the femur is most commonly affected (15–23%), followed by the ribs (12–23%), pelvis (10–13%), humerus (4–16%), tibia (4–6%) and fibula (5%) [5]. Multicentric involvement has been reported in 7% of

cases and rarely, mesenchymal CS may arise secondarily in lesions such as fibrous dysplasia.

Mesenchymal CS, being a high-grade tumour, requires wide excision [2]. The additional benefit from chemotherapy is unclear [39] and a 5-year survival rate of 52% is reported [19].

The imaging features are more aggressive than those of conventional CS (Fig. 15), showing areas of moth-eaten or permeative bone destruction and associated poorly defined periosteal reaction. Typical chondroid matrix mineralisation is reported in two thirds of cases and large extraosseous tumour masses are common. Pathological fracture is infrequent.

The CT features are non-specific (Fig. 16a), being those of an aggressive malignant bone tumour, although subtle matrix mineralisation may point to the diagnosis. The MRI features also differ from those of conventional CS, the lesion typically showing heterogeneous intermediate T2W SI (Fig. 16b), rather than the typical marked hyperintensity of hyaline cartilage. Serpentine signal voids may be seen (Fig. 16b) and the tumour shows either uniform or heterogeneous enhancement following contrast medium administration, rather than the characteristic septal and peripheral enhancement of conventional low-grade CS [5].

Dedifferentiated chondrosarcoma

Dedifferentiated chondrosarcoma (DD-CS) represents approximately 11% of central CS and is defined by the development of a high-grade, non-cartilaginous sarcoma in association with a pre-existing low to intermediate grade CS [40]. The non-cartilaginous lesion is most commonly conventional high-grade osteosarcoma (OS-70%) and less commonly fibrosarcoma or malignant fibrous histiocytoma (MFH) [41]. Rarely, dedifferentiation to leiomyosarcoma [40], telangiectatic OS [40, 42] and giant cell tumour (GCT) [43] has been reported.

The mean age at diagnosis is 59–66 years with equal frequency in males and females [44]. The femur (55%), pelvis (23%) and humerus (10%) are the commonest locations, but the ribs, scapula, tibia and fibula may also be affected. The vast majority of DD-CS arise centrally, but have also rarely been described in association with peripheral CS. Almost one-third of long bone lesions will present with pathological fracture and one-fifth with metastatic disease [44].

Management is with wide local resection and limb salvage where possible, but the use of neoadjuvant chemotherapy should be considered in younger patients, although no definite benefit has been identified [44, 45]. Overall 5-year survival is reported at 24%, with pathological fracture, pelvic location, increasing age and

Fig. 7 Central grade 2 chondrosarcoma. **a** AP radiograph of the proximal femur shows a central chondrosarcoma with extensive cortical thickening (*arrows*). **b** 99m-Tc MDP bone scan shows extensive increased radioisotope uptake in the left proximal femur, which is greater than the tracer uptake in the iliac crest. **c** Coronal T1W FSE MR image of the left femur demonstrates marked cortical hyperostosis (*arrow*). **d** Axial PDW FSE MR image demonstrates cortical penetration with soft tissue extension (*arrows*)



metastases at presentation being associated with a poorer prognosis [44]. The importance of accurate pre-treatment

diagnosis of dedifferentiation has been highlighted in order to optimise treatment and outcome [46].

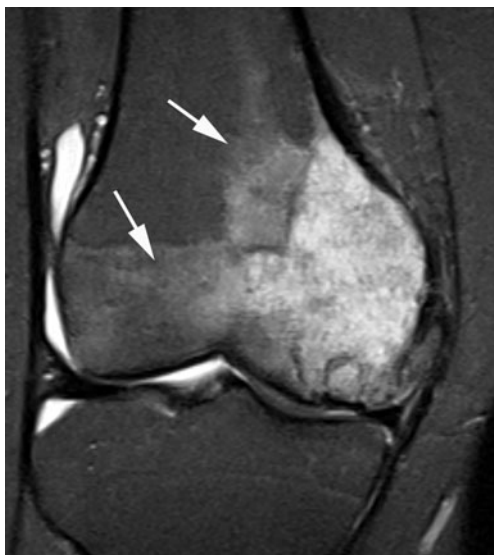


Fig. 8 Grade 2 intramedullary chondrosarcoma. Coronal fat-suppressed PDW FSE MR image shows marked peri-lesional marrow oedema-like signal intensity (*arrows*)

The radiological features are predominantly those of a high-grade CS in 85% of cases, the appearance being consistent with a low-grade CS in 4% of cases [40]. The absence of any radiographic evidence of an underlying chondral tumour is reported in 13%, the lesions having the appearance of non-specific malignant tumours. Radiographic characteristics of primary osteosarcoma may also be seen in 6% [40].

With regard to specific radiographic findings, cortical thickening, endosteal scalloping and periostitis are reported in 32%, 67% and 42% of cases respectively (Fig. 17) [40]. The periosteal reaction is typically solid and “benign” appearing, while multilaminated or spiculated “aggressive” periostitis is seen in ~6% (Fig. 17b, c). Cortical destruction is very common, and is seen on ~60% of radiographs (Fig. 18) and 90% of CT/MRI

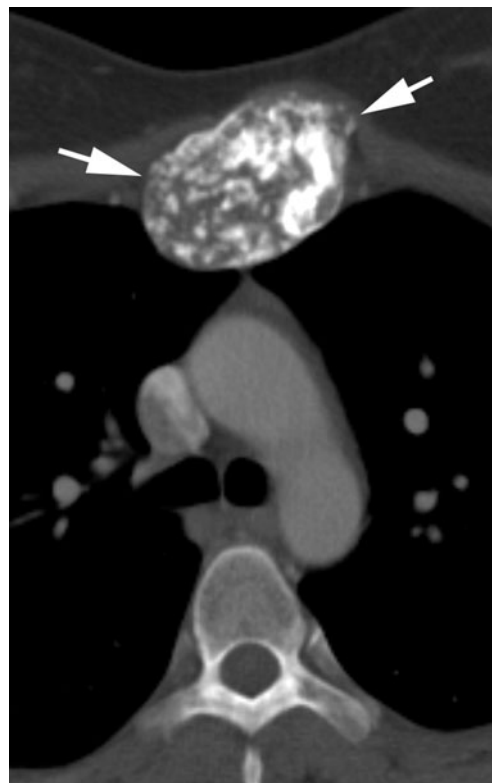


Fig. 10 Chondrosarcoma of the sternum. Axial chest CT shows an expansile lesion (*arrows*) in the sternum, which demonstrates typical chondral-type matrix mineralisation

studies, while pathological fracture is reported in 36% [40]. Chondral matrix mineralisation is evident on 77–82% of radiographs (Fig. 17a, b) or CT, while MRI shows the typical features of chondral tumour morphology and SI characteristics in the majority of cases, even when this is not evident radiographically. A soft-tissue mass may be identified on 25% of radiographs (Fig. 17b) and ~80% of CT/MRI studies (Figs. 17c, 18b, c) [40].

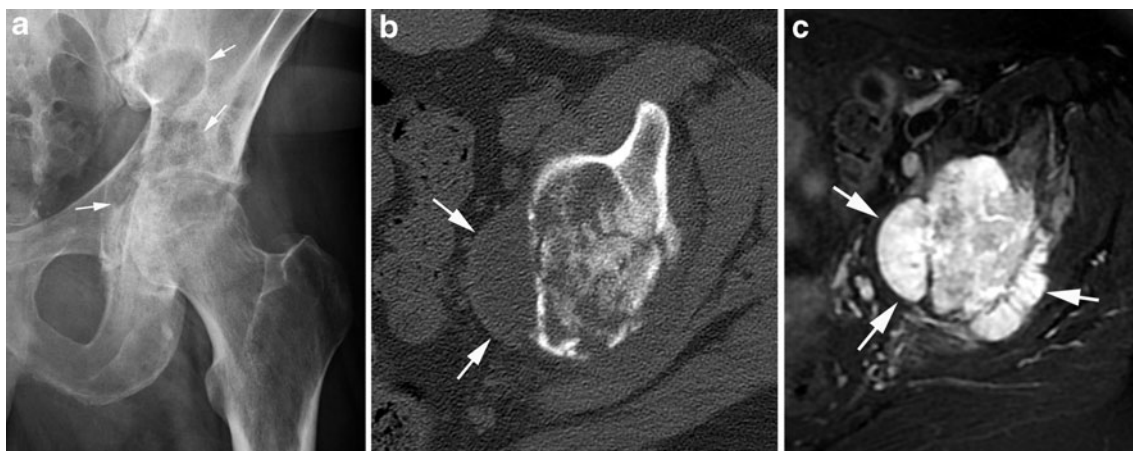


Fig. 9 Central chondrosarcoma of the pelvis. **a** AP radiograph of the left hip demonstrates a lytic, destructive lesion (*arrows*) within the acetabulum at the site of the fused tri-radiate cartilage. **b** Axial CT shows the destructive lesion with soft-tissue extension within the

obturator internus (*arrows*). **c** Axial fat-suppressed T2W FSE MR image shows the lesion within the acetabulum and clearly demonstrates the degree of soft-tissue extension (*arrows*)

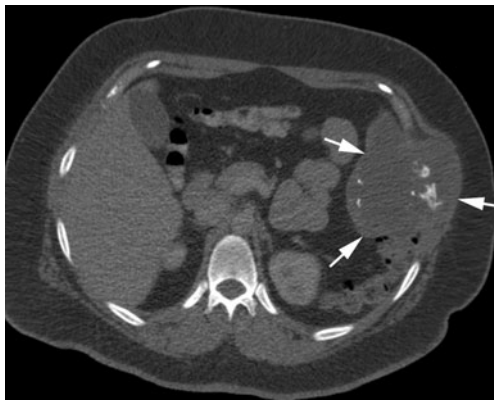


Fig. 11 Chondrosarcoma of the rib. Axial chest CT demonstrates a very extensive chondral lesion that is causing rib destruction and shows a very extensive soft-tissue component (*arrows*)

The key to the diagnosis of DD-CS is the demonstration of tumour bi-morphism, this being the presence of a chondral and a non-chondral component to the lesion. Radiologically, this may manifest as an area of aggressive bone destruction, with/without osseous-type tumour matrix adjacent to an area of typical chondral tumour [40] (Fig. 17). MRI can accurately identify tumour bi-morphism based predominantly on T2W FSE and post-gadolinium T1W SE images [47]. On T2W FSE MRI, well-differentiated chondral tumour appears lobular and markedly hyperintense,

Fig. 12 Grade 2 chondrosarcoma of the proximal phalanx of the little finger. **a** AP radiograph shows a permeative lytic lesion with cortical destruction (*arrows*). **b** Coronal T2W FSE MR image shows extensive cortical destruction and lobular soft tissue extension (*arrows*)



Fig. 13 Chondrosarcoma of the calcaneus. Lateral radiograph of the ankle shows a very large lesion arising from the inferior calcaneus with marked soft-tissue extension and chondral-type matrix mineralisation (*arrows*)

showing a combination of peripheral/septal enhancement on T1W SE images following gadolinium (see above). Features indicative of DD-CS include the presence of an adjacent tumour mass with relatively lower T2W SI (Fig. 19) and uniform contrast enhancement, representing the high-grade sarcoma. This bi-morphic pattern was identified in 6/8 DD-CS (75%) [47] and has been shown to be of value in targeting the high-grade region at time of image-

Fig. 14 Clear cell chondrosarcoma. **a** AP radiograph of the left hip shows a predominantly lytic lesion (arrows) in the femoral head with a poorly-defined, thin sclerotic margin. **b** CT of the left hip clearly depicts the degree of matrix mineralisation and the sclerotic margin of the lesion (arrows). **c** Coronal T1W SE and **d** coronal fat-suppressed T2W FSE MR images show the lesion to be of low-intermediate SI on T1W and of heterogeneous increased SI on the fat-suppressed T2W sequence. Note the subtle marginal sclerosis of the lesion (arrows) and the absence of reactive medullary oedema and synovitis



guided needle biopsy [48]. Less common MRI patterns include a lesion that has imaging features of a high-grade

sarcoma, the only indication of an underlying chondral tumour being the presence of punctate/curvilinear signal

Fig. 15 Mesenchymal chondrosarcoma. **a** AP and **b** lateral radiographs of the knee show a predominantly lytic, lobular lesion in the proximal tibia (arrows) with apparent internal trabeculation

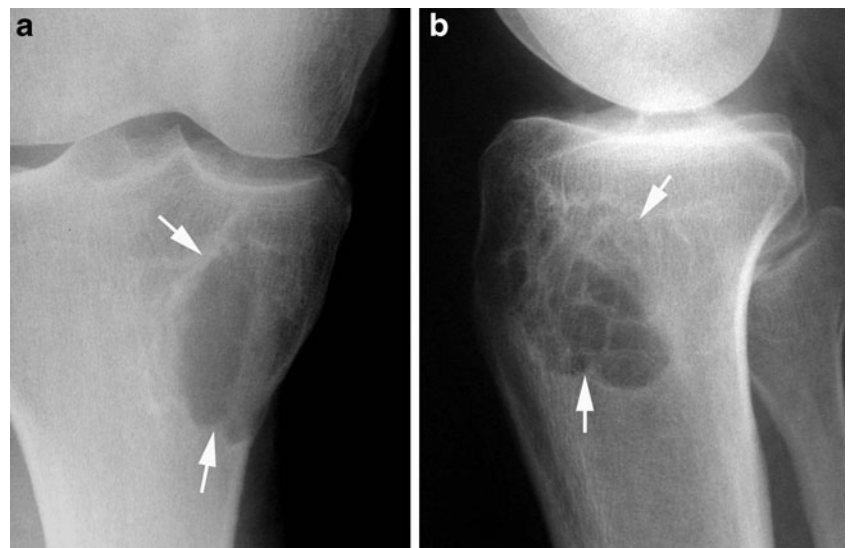
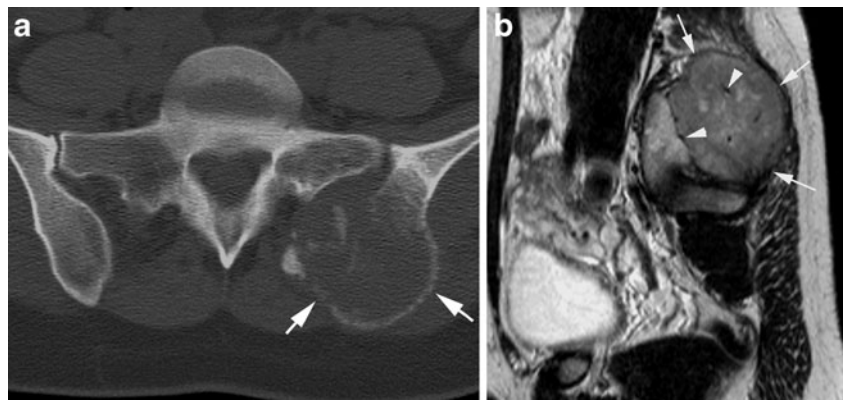


Fig. 16 Mesenchymal chondrosarcoma. **a** Axial CT of the pelvis shows an ill-defined, aggressive, expansile lesion in the left posterior ilium (*arrows*), which has caused cortical destruction and soft tissue extension. **b** Sagittal T2W FSE MR image demonstrates the lesion to be of heterogeneous intermediate signal intensity (*arrows*). Note the multiple serpentine signal voids within the lesion (*arrowheads*)



voids due to residual chondral matrix mineralisation. Alternatively, in the absence of such matrix mineralisation, a non-specific MR appearance may be seen (Fig. 18b, c) [47].

Periosteal chondrosarcoma

Periosteal chondrosarcoma (periosteal CS) is also termed juxta-cortical or parosteal CS, as it is a lesion that arises on the surface of the bone [5, 49–51]. It is a rare tumour accounting for ~0.2% of bone tumours [49] and ~4% of all CS [5]. It usually presents in adults in the 3rd to 4th decades

with a non-specific, slowly growing painless/painful mass. Based on a combination of 59 cases from the literature [50–52], 29 (49%) were located in the femur, 14 (24%) in the humerus and 8 (14%) in the tibia, with rarely reported sites including the ilium, fibula and rib. The majority of cases involve low-grade tumours, which are adequately treated by wide excision. An overall disease-free 5-year survival of 83% is reported [52].

The lesion is located on the long bone surface, usually in a metaphyseal or metadiaphyseal region, and varies in size from 3 to 14 cm [50, 51]. Thickening or thinning of the underlying cortex is almost invariable, but complete cortical

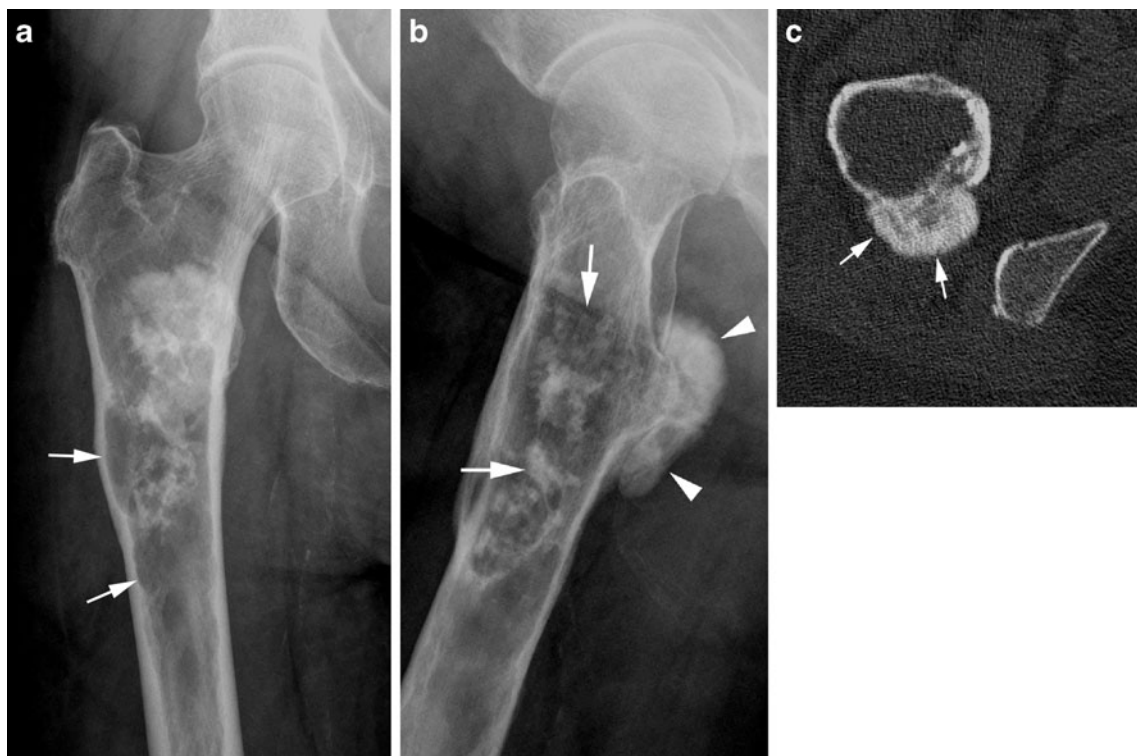


Fig. 17 Dedifferentiated chondrosarcoma. **a** AP radiograph of the femur shows an extensive, poorly-defined mixed lytic and sclerotic lesion in the proximal femur, which demonstrates endosteal scalloping (*arrows*). **b** Lateral radiograph of the proximal femur reveals the chondral-type mineralization in the intramedullary component of the

lesion (*arrows*) and the densely osteoblastic mineralization of the dedifferentiated component (*arrowheads*). **c** Axial CT of the femur clearly depicts the densely osteoblastic posterior soft-tissue mass (*arrows*)



Fig. 18 Dedifferentiated chondrosarcoma of the acetabulum. **a** AP radiograph of the right hip shows a poorly-defined lesion that has destroyed the medial acetabular wall (*arrow*) with soft tissue extension. **b** Coronal

T1W and **c** axial T2W FSE MR images show a lesion with no specific SI characteristics and no evidence of an underlying chondral origin (*arrows*)

destruction is not a feature [51]. Chondral-type matrix mineralisation is present in the majority of cases (Fig. 20a).

On CT, a thin peripheral calcified margin is present in ~50% of cases. On MRI, a lobular growth pattern typical of low-grade chondral tumours is a characteristic feature, with the lesion showing low to intermediate T1W SI and increased T2W SI (Fig. 20b), as expected [50]. Surrounding reactive oedema-like changes in either the underlying bone or the adjacent soft tissues are uncommon findings [50], while histologically proven marrow involvement was demonstrated in 4 out of 25 cases [50, 51].

The imaging features alone do not adequately distinguish between periosteal chondrosarcoma and periosteal chondroma, the major differentiation being lesion size, with chondroma having a mean size of 2.2 cm (range 1–6.5 cm) and chondrosarcoma having a mean size of 5.3 cm (range 3–

14 cm) [50]. Periosteal chondroma tends to be painless and is usually seen in younger patients [53]. The lesion also has to be differentiated from periosteal osteosarcoma, which typically affects patients in the second and third decades of life and on radiographs demonstrates a juxta-cortical soft-tissue mass, a large amount of cortical erosion and a perpendicular periosteal reaction [53].

Secondary chondrosarcoma

As previously stated, a secondary CS is one that develops in association with an underlying benign chondral lesion, either enchondroma (single or multiple) or osteochondroma (OC; single or multiple) [6–9]. Secondary CS developing from an underlying enchondroma has already been dealt with in the

Fig. 19 Dedifferentiated chondrosarcoma of the femur. **a** Axial T2W FSE and **b** coronal STIR MR images demonstrate a hyperintense intramedullary lesion (*arrows*) with an adjacent intermediate SI mass (*arrowhead*) consistent with the dedifferentiated component

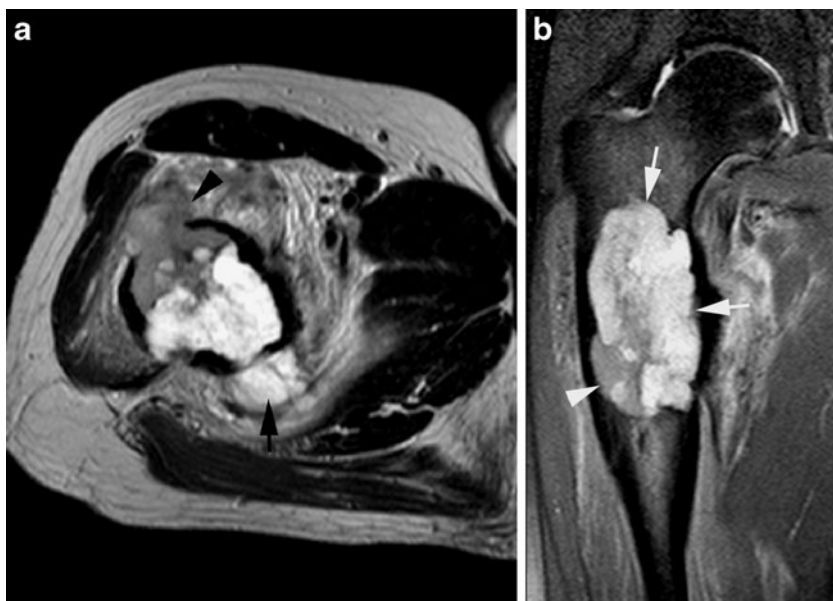


Fig. 20 Periosteal chondrosarcoma. **a** Lateral radiograph of the knee shows a predominantly lytic lesion with chondral-type matrix mineralisation (*arrow*) arising from the posterior surface of the distal femur. Note the associated cortical thickening. **b** Sagittal T2W FSE MR image demonstrates the lesion (*arrows*) to be of predominantly increased SI with a typical lobular morphology



first part of this series, as it has similar characteristics to primary conventional central CS, whilst an in-depth discussion of secondary CS developing in association with skeletal dysplasias, such as Ollier's disease, Maffucci syndrome and diaphyseal aclasis, is outside the remit of this review article.

Secondary CS arising from a solitary OC (also termed peripheral CS) is reported to occur in ~4% of cases [7, 49]. However, considering that many OCs are asymptomatic or treated conservatively, the overall transformation rate is estimated at closer to 1% [54]. Transformation occurs in the cartilaginous component of the lesion, the vast majority being low-grade CS [49, 54], while transformation to DD-CS is also occasionally reported [55]. Secondary CS due to solitary osteochondroma usually presents at 50–55 years of age [54]. Clinical symptoms include new or increasing pain and an enlarging mass. The commonest sites of occurrence are the pelvis, around the hip joint and the shoulder girdle.

Since malignancy occurs in the cartilage cap, the diagnosis depends greatly upon an estimation of cartilage cap thickness [54, 56, 57]. Radiographic features suggestive of malignancy include growth of an OC in a skeletally mature patient, an irregular/indistinct lesion surface, focal areas of lysis within the osseous component of the lesion, erosion/destruction of the adjacent bone and a large soft-tissue mass containing scattered chondral-type calcifications (Fig. 21a) [54].

99m -technetium MDP bone scintigraphy does not allow the differentiation of benign from malignant OC and a normal bone scan does not exclude malignant transformation [54]. However, it has been suggested that PET may play a role in identifying such change based on increased metabolic activity within a malignant cartilage cap [58].

Cartilage cap thickness can be assessed with ultrasound, CT and MRI [54, 57]. Cap thickness in benign OC can range from 0.1 to 3.0 cm (mean 0.6–0.8 cm), while that for

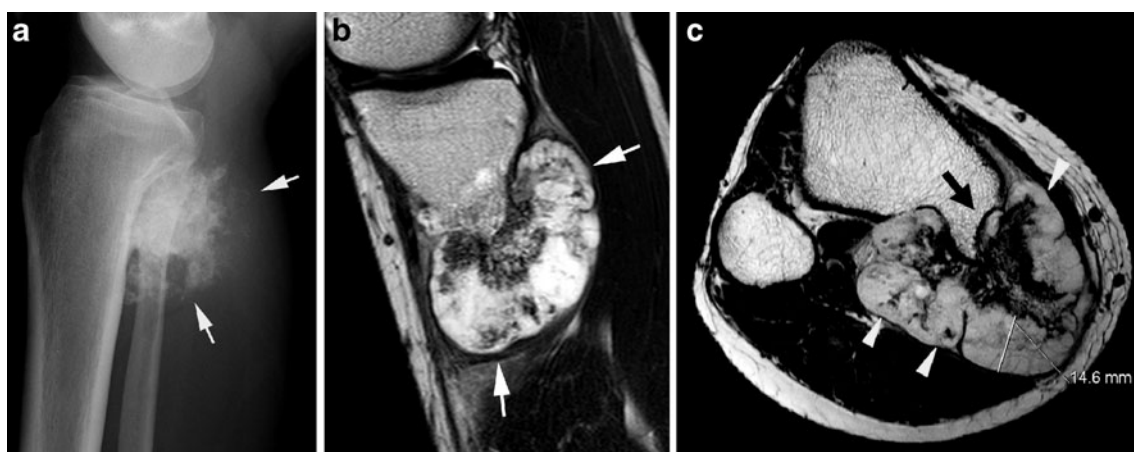


Fig. 21 Secondary chondrosarcoma of the tibia. **a** Lateral radiograph of the tibia demonstrates a large soft-tissue mass with extensive chondral-type matrix mineralisation adjacent to the posterior proximal tibial cortex. **b** Sagittal T2W FSE MR image shows the markedly hyperintense cartilage cap (*arrows*) as well as areas of signal void

due to matrix mineralisation. **c** Axial PDW FSE MR image clearly depicts the stalk of the osteochondroma (*black arrow*), the lobular appearance of the cartilage cap (*white arrows*), the cartilage cap thickness and areas of signal void due to matrix mineralisation

secondary CS has been reported to be 1.5–12 cm (mean 5.5–6.0 cm). Therefore, a cartilage cap thickness ranging from 1 to 3 cm has been thought to be suspicious for malignant transformation into a chondrosarcoma [54, 59]. However, this wide range in cartilage cap thickness may be due to different measurement techniques in convoluted cartilage caps [59]. Recently, Bernard et al. validated a technique for the measurement of the cartilage cap of osteochondromas on CT and MRI and correlated the radiological findings with the pathology specimen. The authors concluded that a cartilage cap thickness of 2 cm or greater strongly indicated malignant transformation into chondrosarcoma [59].

The MRI appearance of the cartilage cap is as would be expected for well-differentiated hyaline chondral tissue, i.e. relatively hypointense to muscle on T1W SE images, markedly hyperintense on T2W FSE (Fig. 21b) and STIR, and showing a combination of peripheral and septal enhancement following intravenous gadolinium. Matrix mineralisation appears as punctate/curvilinear areas of signal void and a lobular growth pattern is classical (Fig. 21c) [56, 57].

Conclusion

Chondrosarcoma is the third most common primary malignant bone tumour after multiple myeloma and osteosarcoma. The vast majority are conventional intramedullary chondrosarcomas whilst clear cell, mesenchymal and dedifferentiated chondrosarcomas represent rare forms of the lesion. The different histological subtypes, histological grading and the different location of chondrosarcoma lead to heterogeneity of the imaging appearance. However, there are specific imaging features that aid in the differentiation between chondrosarcoma and other bone neoplasms and in the characterisation of the various subtypes. Knowledge of these characteristics leads to increased diagnostic accuracy, may guide biopsy and ultimately improve overall patient care.

References

- Brien EW, Mirra JM, Kerr R. Benign and malignant cartilage tumors of bone and joint: their anatomic and theoretical basis with an emphasis on radiology, pathology and clinical biology. I. The intramedullary cartilage tumors. *Skeletal Radiol*. 1997;26:325–53.
- Marco RA, Gitelis S, Brebach GT, Healey JH. Cartilage tumors: evaluation and treatment. *J Am Acad Orthop Surg*. 2000;8:292–304.
- Flemming DJ, Murphey MD. Enchondroma and chondrosarcoma. *Semin Musculoskelet Radiol*. 2000;4:59–71.
- Aigner T. Towards a new understanding and classification of chondrogenic neoplasias of the skeleton—biochemistry and cell biology of chondrosarcoma and its variants. *Virchows Arch*. 2002;441:219–30.
- Murphey MD, Walker EA, Wilson AJ, Kransdorf MJ, Temple HT, Gannon FH. From the archives of the AFIP: imaging of primary chondrosarcoma: radiologic–pathologic correlation. *Radiographics*. 2003;23:1245–78.
- Ahmed AR, Tan TS, Unni KK, Collins MS, Wenger DE, Sim FH. Secondary chondrosarcoma in osteochondroma: report of 107 patients. *Clin Orthop Relat Res*. 2003;193–206.
- Altay M, Bayrakci K, Yildiz Y, Ereku S, Saglik Y. Secondary chondrosarcoma in cartilage bone tumors: report of 32 patients. *J Orthop Sci*. 2007;12:415–23.
- Bovee JV, van Roggen JF, Cleton-Jansen AM, Taminiau AH, van der Woude HJ, Hogendoorn PC. Malignant progression in multiple enchondromatosis (Ollier's disease): an autopsy-based molecular genetic study. *Hum Pathol*. 2000;31:1299–303.
- Shah ZK, Peh WC, Wong Y, Shek TW, Davies AM. Sarcomatous transformation in diaphyseal acclasis. *Australas Radiol*. 2007;51:110–9.
- Skeletal Lesions Interobserver Correlation among Expert Diagnosticians (SLICED) Study Group. Reliability of histopathologic and radiologic grading of cartilaginous neoplasms in long bones. *J Bone Joint Surg Am*. 2007;89:2113–23.
- Eefting D, Schrage YM, Geirmaerd MJ, Le Cessie S, Taminiau AH, Bovee JV, et al. Assessment of interobserver variability and histologic parameters to improve reliability in classification and grading of central cartilaginous tumors. *Am J Surg Pathol*. 2009;33:50–7.
- Reith JD, Horodyski MB, Scarborough MT. Grade 2 chondrosarcoma: stage I or stage II tumor? *Clin Orthop Relat Res*. 2003;45–51.
- O'Connor MI, Bancroft LW. Benign and malignant cartilage tumors of the hand. *Hand Clin*. 2004;20:317–23. vi.
- Patil S, de Silva MV, Crossan J, Reid R. Chondrosarcoma of the bones of the feet. *J Foot Ankle Surg*. 2003;42:290–5.
- Duarte MP, Maldjian C, Katta US, Kenan S. Conventional intramedullary chondrosarcoma with subarticular involvement. *Clin Imaging*. 2008;32:69–72.
- Douis H, James SL, Grimer RJ, Davies MA. Is bone scintigraphy necessary in the initial surgical staging of chondrosarcoma of bone? *Skeletal Radiol*. 2012;41:429–36.
- Leerapun T, Hugate RR, Inwards CY, Scully SP, Sim FH. Surgical management of conventional grade I chondrosarcoma of long bones. *Clin Orthop Relat Res*. 2007;463:166–72.
- Jones K, Pacella J, Kirby AD, Pervez N. Unusual behaviour of low-grade chondrosarcoma of bone. *J Med Imaging Radiat Oncol*. 2008;52:95–6.
- Damron TA, Ward WG, Stewart A. Osteosarcoma, chondrosarcoma, and Ewing's sarcoma: National Cancer Data Base report. *Clin Orthop Relat Res*. 2007;459:40–7.
- Schwab JH, Wenger D, Unni K, Sim FH. Does local recurrence impact survival in low-grade chondrosarcoma of the long bones? *Clin Orthop Relat Res*. 2007;462:175–80.
- Fong YC, Pairolo PC, Sim FH, Cha SS, Blanchard CL, Scully SP. Chondrosarcoma of the chest wall: a retrospective clinical analysis. *Clin Orthop Relat Res*. 2004;184–9.
- Pant R, Yasko AW, Lewis VO, Raymond K, Lin PP. Chondrosarcoma of the scapula: long-term oncologic outcome. *Cancer*. 2005;104:149–58.
- Jawad MU, Haleem AA, Scully SP. Malignant sarcoma of the pelvic bones: treatment outcomes and prognostic factors vary by histopathology. *Cancer*. 2011;117:1529–41.
- Pring ME, Weber KL, Unni KK, Sim FH. Chondrosarcoma of the pelvis. A review of sixty-four cases. *J Bone Joint Surg Am*. 2001;83-A:1630–42.
- Schneiderbauer MM, Blanchard C, Gullerud R, Harmsen WS, Rock MG, Shives TC, et al. Scapular chondrosarcomas have high rates of local recurrence and metastasis. *Clin Orthop Relat Res*. 2004;232–8.
- Giuffrida AY, Burgueno JE, Koniaris LG, Gutierrez JC, Duncan R, Scully SP. Chondrosarcoma in the United States (1973 to 2003): an

- analysis of 2890 cases from the SEER database. *J Bone Joint Surg Am.* 2009;91:1063–72.
27. Bramer JA, Abudu AA, Grimer RJ, Carter SR, Tillman RM. Do pathological fractures influence survival and local recurrence rate in bony sarcomas? *Eur J Cancer.* 2007;43:1944–51.
 28. Ehara S, Nakayama T, Nishida J, Shiraiishi H, Yoshioka H, Aoki J. Bone scintigraphic and CT evaluation of chondrosarcoma of the rib: correlation with histological grade in 6 cases. *Ann Nucl Med.* 2004;18:633–6.
 29. Feldman F, Van Heertum R, Saxena C, Parisien M. 18FDG-PET applications for cartilage neoplasms. *Skeletal Radiol.* 2005;34:367–74.
 30. Brenner W, Conrad EU, Eary JF. FDG PET imaging for grading and prediction of outcome in chondrosarcoma patients. *Eur J Nucl Med Mol Imaging.* 2004;31:189–95.
 31. Yoo HJ, Hong SH, Choi JY, Moon KC, Kim HS, Choi JA, et al. Differentiating high-grade from low-grade chondrosarcoma with MR imaging. *Eur Radiol.* 2009;19:3008–14.
 32. Collins MS, Koyama T, Swee RG, Inwards CY. Clear cell chondrosarcoma: radiographic, computed tomographic, and magnetic resonance findings in 34 patients with pathologic correlation. *Skeletal Radiol.* 2003;32:687–94.
 33. Itala A, Leerapun T, Inwards C, Collins M, Scully SP. An institutional review of clear cell chondrosarcoma. *Clin Orthop Relat Res.* 2005;440:209–12.
 34. Donati D, Yin JQ, Colangeli M, Colangeli S, Bella CD, Bacchini P, et al. Clear cell chondrosarcoma of bone: long time follow-up of 18 cases. *Arch Orthop Trauma Surg.* 2008;128:137–42.
 35. Kaim AH, Hugli R, Bonel HM, Jundt G. Chondroblastoma and clear cell chondrosarcoma: radiological and MRI characteristics with histopathological correlation. *Skeletal Radiol.* 2002;31:88–95.
 36. Memis A, Arkun R, Basdemir G, Sabah D, Ustun EE. Clear cell chondrosarcoma: unusual radiologic appearances with histologic correlation. *Eur Radiol.* 2002;12:427–30.
 37. Corradi D, Bacchini P, Campanini N, Bertoni F. Aggressive clear cell chondrosarcomas: do distinctive characteristics exist?: a report of 4 cases. *Arch Pathol Lab Med.* 2006;130:1673–9.
 38. Kalil RK, Inwards CY, Unni KK, Bertoni F, Bacchini P, Wenger DE, et al. Dedifferentiated clear cell chondrosarcoma. *Am J Surg Pathol.* 2000;24:1079–86.
 39. Cesari M, Bertoni F, Bacchini P, Mercuri M, Palmerini E, Ferrari S. Mesenchymal chondrosarcoma. An analysis of patients treated at a single institution. *Tumori.* 2007;93:423–7.
 40. Littrell LA, Wenger DE, Wold LE, Bertoni F, Unni KK, White LM, et al. Radiographic, CT, and MR imaging features of dedifferentiated chondrosarcomas: a retrospective review of 174 de novo cases. *Radiographics.* 2004;24:1397–409.
 41. Staals EL, Bacchini P, Bertoni F. Dedifferentiated central chondrosarcoma. *Cancer.* 2006;106:2682–91.
 42. Okada K, Hasegawa T, Tateishi U, Endo M, Itoi E. Dedifferentiated chondrosarcoma with telangiectatic osteosarcoma-like features. *J Clin Pathol.* 2006;59:1200–2.
 43. Estrada EG, Ayala AG, Lewis V, Czerniak B. Dedifferentiated chondrosarcoma with a noncartilaginous component mimicking conventional giant cell tumor of bone. *Ann Diagn Pathol.* 2002;6:159–63.
 44. Grimer RJ, Gosheger G, Taminiau A, Biau D, Matejovsky Z, Kollender Y, et al. Dedifferentiated chondrosarcoma: prognostic factors and outcome from a European group. *Eur J Cancer.* 2007;43:2060–5.
 45. Dickey ID, Rose PS, Fuchs B, Wold LE, Okuno SH, Sim FH, et al. Dedifferentiated chondrosarcoma: the role of chemotherapy with updated outcomes. *J Bone Joint Surg Am.* 2004;86-A:2412–8.
 46. Mitchell AD, Ayoub K, Mangham DC, Grimer RJ, Carter SR, Tillman RM. Experience in the treatment of dedifferentiated chondrosarcoma. *J Bone Joint Surg Br.* 2000;82:55–61.
 47. MacSweeney F, Darby A, Saifuddin A. Dedifferentiated chondrosarcoma of the appendicular skeleton: MRI-pathological correlation. *Skeletal Radiol.* 2003;32:671–8.
 48. Saifuddin A, Mann BS, Mahroof S, Pringle JA, Briggs TW, Cannon SR. Dedifferentiated chondrosarcoma: use of MRI to guide needle biopsy. *Clin Radiol.* 2004;59:268–72.
 49. Brien EW, Mirra JM, Luck Jr JV. Benign and malignant cartilage tumors of bone and joint: their anatomic and theoretical basis with an emphasis on radiology, pathology and clinical biology. II. Juxtacortical cartilage tumors. *Skeletal Radiol.* 1999;28:1–20.
 50. Robinson P, White LM, Sundaram M, Kandel R, Wunder J, McDonald DJ, et al. Periosteal chondroid tumors: radiologic evaluation with pathologic correlation. *AJR Am J Roentgenol.* 2001;177:1183–8.
 51. Vanel D, De Paolis M, Monti C, Mercuri M, Picci P. Radiological features of 24 periosteal chondrosarcomas. *Skeletal Radiol.* 2001;30:208–12.
 52. Papagelopoulos PJ, Galanis EC, Mavrogenis AF, Savvidou OD, Bond JR, Unni KK, et al. Survivorship analysis in patients with periosteal chondrosarcoma. *Clin Orthop Relat Res.* 2006;448:199–207.
 53. Chaabane S, Bouaziz MC, Drissi C, Abid L, Ladeb MF. Periosteal chondrosarcoma. *AJR Am J Roentgenol.* 2009;192:W1–6.
 54. Murphey MD, Choi JJ, Kransdorf MJ, Flemming DJ, Gannon FH. Imaging of osteochondroma: variants and complications with radiologic-pathologic correlation. *Radiographics.* 2000;20:1407–34.
 55. Staals EL, Bacchini P, Mercuri M, Bertoni F. Dedifferentiated chondrosarcomas arising in preexisting osteochondromas. *J Bone Joint Surg Am.* 2007;89:987–93.
 56. Lee KC, Davies AM, Cassar-Pullicino VN. Imaging the complications of osteochondromas. *Clin Radiol.* 2002;57:18–28.
 57. Woertler K, Lindner N, Gosheger G, Brinkschmidt C, Heindel W. Osteochondroma: MR imaging of tumor-related complications. *Eur Radiol.* 2000;10:832–40.
 58. Feldman F, Vanheertum R, Saxena C. 18fluoro-deoxyglucose positron emission tomography evaluation of benign versus malignant osteochondromas: preliminary observations. *J Comput Assist Tomogr.* 2006;30:858–64.
 59. Bernard SA, Murphey MD, Flemming DJ, Kransdorf MJ. Improved differentiation of benign osteochondromas from secondary chondrosarcomas with standardized measurement of cartilage cap at CT and MR imaging. *Radiology.* 2010;255:857–65.